J. Fluid Mech. (1984), *vol.* 149, *pp.* 147–159
Printed in Great Britain

Turbulent dispersion from a steady two-dimensional horizontal source

By R. I. NOKES,
Department of Civil Engineering, University of Canterbury, Christchurch, New Zealand

A. J. McNULTY
Hydrology Centre, Ministry of Works and Development, Christchurch, New Zealand

AND I. R. WOOD
Department of Civil Engineering, University of Canterbury, Christchurch, New Zealand

(Received 12 December 1983 and in revised form 22 May 1984)

The two-dimensional steady-state turbulent-diffusion equation is solved by a separation-of-variables process that leads to a Sturm–Liouville eigenvalue problem. The general solution, for arbitrary velocity and diffusivity distributions, is shown to be in the form of an eigenfunction expansion. For a steady uniform flow in a wide, open channel the velocity distribution in the vertical is well approximated by a logarithmic law and the diffusivity distribution is approximately parabolic. For these distributions the power-series solution technique for ordinary differential equations is used to determine the eigenfunctions and eigenvalues. The solution is compared with the standard solution that Holley, Siemans & Abraham (1972) obtained for a uniform velocity and diffusivity distribution. Experimental results are presented, and these show that

(1) the use of the correct velocity and diffusivity distribution results in a significant improvement in the agreement between experiment and theory; and

(2) close to the source the fluctuations of concentration are of the order of the mean values.

1. Introduction

The dispersion of an instantaneous release of a slug of pollutant has received considerable attention and has been studied both theoretically and experimentally. Equally important is the dispersion of effluent from a continuous source, such as would occur from a factory outfall. Such a source may be treated as steady provided that any changes with time are small over the period of time an average particle takes to travel downstream from the source to the uniformly mixed region.

In order to solve this problem for vertical dispersion Holley, Siemans & Abraham (1972), Fischer *et al.* (1979) and others have made the assumption that longitudinal concentration gradients are small compared with vertical concentration gradients, and this has enabled analytic solutions to be obtained for a uniform velocity and diffusivity distribution (Holley *et al.* 1972) and for a power-law velocity and diffusivity distribution (Yeh & Tsai 1976). The measured velocity distribution, however, is, except near the bed, approximately logarithmic, and this implies a parabolic distribution of diffusivity. No analytic solution is available for these distributions. McNulty & Wood (1984) approached this problem by adapting Aris'

method of moments to a continuous release, and were able to generate the required solution far from the source. Coudert (1970), on the other hand, solved the problem numerically by using a Crank–Nicholson finite-difference scheme. However, his final results are inconsistent with his stated boundary conditions.

In this paper the dispersion equation is reduced to an eigenvalue problem, following the approach used by Smith (1982), and a general form of the solution, for any choice of velocity and diffusivity distributions, is given in §3. In §4 the eigenfunctions and eigenvalues for a logarithmic velocity and parabolic diffusivity are derived by employing the power-series method of solution for ordinary differential equations. Details of the numerical calculations are included in §5 together with the numerical results. Concentration contours for constant velocity and diffusivity distributions are compared with those for a logarithmic velocity and parabolic diffusivity distributions. Some experimental results are presented in §6.

2. Development of the equations

The process of two-dimensional turbulent diffusion of a conservative neutrally buoyant substance in steady flow is generally modelled by the equation

$$u\frac{\partial c}{\partial x} = \frac{\partial}{\partial x}\left(\epsilon_x \frac{\partial c}{\partial x}\right) + \frac{\partial}{\partial y}\left(\epsilon_y \frac{\partial c}{\partial y}\right), \tag{1}$$

where the flow is taken to be in the positive x-direction and y is measured vertically from the bed. ϵ_x and ϵ_y are the turbulent diffusion coefficients in the x- and y-directions respectively, u is the x-component of the mean velocity and c is the mean concentration of the dispersing material. The Fickian form of (1) comes from the assumption that the turbulent transport terms are proportional to the mean concentration gradients. This form is particularly convenient for a two-dimensional flow, since the distribution of ϵ_y can be determined from the hydraulic properties and the Reynolds analogy.

For the flow in a long wide uniform channel the flow depth y_n and all the mean flow variables (ϵ_x, ϵ_y and u) will not be functions of x.

To obtain a particular solution to (1), boundary conditions must also be specified. The boundary conditions require no vertical flux of material across the bed and free surface and a certain concentration configuration, source condition, specified at some section in the flow. These conditions may be stated as

$$\epsilon_y \frac{\partial c}{\partial y} = 0 \quad \text{at} \quad y = 0, y_n \tag{2}$$

and

$$c(0, y) = c_s(y). \tag{3}$$

Provided that the longitudinal concentration gradients are negligible compared with the vertical gradients, as demonstrated by McNulty & Wood (1984), (1) reduces to

$$u(y)\frac{\partial c}{\partial x} = \frac{\partial}{\partial y}\left[\epsilon_y(y)\frac{\partial c}{\partial y}\right]. \tag{4}$$

Choosing the variables

$$x' = \frac{x}{y_n}, \quad y' = \frac{y}{y_n}, \quad u = \bar{u}\chi(y'), \quad \epsilon_y = D\psi(y'), \tag{5}$$

(4) may be non-dimensionalized. $\bar{u}$ is the depth-averaged velocity, $D = u_*^2 y_n/\bar{u}$, is the diffusivity coefficient $u_* = (\tau_0/\rho)^{\frac{1}{2}}$ is the shear velocity, τ_0 is the bed shear stress and

ρ is the fluid density. $\chi(y')$ is a non-dimensional velocity and $\psi(y')$ is a non-dimensional diffusivity, which, if Reynolds' analogy with the linear shear stress for uniform flow in a wide channel is used, becomes

$$\psi(y') = \frac{1-y'}{\mathrm{d}\chi/\mathrm{d}y'}, \tag{6}$$

If these transformations are applied to (4) and the primes are dropped for clarity, the governing equation becomes

$$\frac{8}{f}\chi(y)\frac{\partial c}{\partial x} = \frac{\partial}{\partial y}\left[\psi(y)\frac{\partial c}{\partial y}\right], \tag{7}$$

where $f = 8(u_*/\bar{u})^2$ and the variables x and y are understood to be dimensionless. Equation (2) becomes

$$\psi(y)\frac{\partial c}{\partial y} = 0 \quad \text{at} \quad y = 0, 1. \tag{8}$$

3. Transformation to a Sturm–Liouville eigenvalue problem

Equation (4) may be transformed to two ordinary differential equations by assuming a separated solution of the form

$$c(x, y) = G(x)\,H(y). \tag{9}$$

The functions $G(x)$ and $H(y)$ satisfy the equations

$$\frac{\mathrm{d}G}{\mathrm{d}x} + \tfrac{1}{8}f\gamma G = 0, \tag{10}$$

$$\frac{\mathrm{d}}{\mathrm{d}y}\left[\psi\frac{\mathrm{d}H}{\mathrm{d}y}\right] + \gamma\chi H = 0, \tag{11}$$

where γ is the constant of separation. Equation (10) has the solution

$$G(x) = A\exp\left[-\tfrac{1}{8}f\gamma x\right], \tag{12}$$

where A is some arbitrary constant, while (11), together with the separated form of (8),

$$\psi\frac{\mathrm{d}H}{\mathrm{d}y} = 0 \quad \text{at} \quad y = 0, 1, \tag{13}$$

constitute an eigenvalue problem governed by Sturm–Liouville theory. With some minor modification, standard proofs (Ince 1927) can be used to demonstrate that the eigenvalues of this problem are real, discrete and non-degenerate and that the eigenfunctions are mutually orthogonal with respect to the weighting function $\chi(y)$ over the interval $0 \leqslant y \leqslant 1$. The eigenfunctions are also assumed to form a complete set, thus allowing any well-behaved (at least piecewise-continuous) function in the interval $0 \leqslant y \leqslant 1$ to be expressed as an infinite series of the eigenfunctions.

The general solution of (7) is given by

$$c(x, y) = \sum_{\gamma} a_\gamma \exp\left[-\tfrac{1}{8}\gamma f x\right] H_\gamma(y), \tag{14}$$

with the sum taken over all possible values of γ satisfying (11) and (13). Only non-negative values of γ will be physically acceptable, with $\gamma = 0$, the smallest

eigenvalue, corresponding to the equilibrium condition when the pollutant is uniformly mixed throughout the flow. The eigenvalues may thus be placed in order of increasing magnitude, and (14) may be written

$$c(x,y) = \sum_{i=0}^{\infty} a_i \exp\left[-\tfrac{1}{8}\gamma_i f x\right] H_i(y). \tag{15}$$

The expansion constants a_i are determined by the source condition (3) at $x = 0$. By virtue of the orthogonality condition

$$a_i = \frac{\int_0^1 c_s(y)\,\chi(y)\,H_i(y)\,\mathrm{d}y}{\int_0^1 \chi(y)\,H_i^2(y)\,\mathrm{d}y} \quad (i = 0, 1, \ldots, \infty). \tag{16}$$

Setting $H_0(y) = 1$ and making use of the definition of $\chi(y)$, the expression for a_0 reduces to

$$a_0 = \int_0^1 c_s(y)\,\chi(y)\,\mathrm{d}y, \tag{17}$$

which is equivalent to the expression for the equilibrium concentration c_e, given by McNulty & Wood (1984). A dimensionless concentration may be defined as

$$c_* = c/a_0, \tag{18}$$

and all numerical and experimental results presented in §§5 and 6 will be displayed in this non-dimensional form.

Equations (15) and (16) represent a complete formal solution to the steady two-dimensional dispersion problem of a continuous pollutant release. The final task is to determine the eigenvalues and eigenfunctions for a particular choice of diffusivity and velocity. This will be done in §4.

4. Power-series solution for calculation of the eigenfunctions and eigenvalues

The eigenfunctions and eigenvalues of (11) and (13) depend on the choice of velocity and diffusivity distributions. By making the approximation that $\chi(y)$ and $\psi(y)$ are constants, (11) and (13) yield the standard analytic solution where the eigenvalues are given by

$$\gamma_m = \psi m^2 \pi^2 \quad (m = 0, 1, \ldots, \infty), \tag{19}$$

in which ψ is the depth-averaged diffusivity, and eigenfunctions are given by

$$H_m = \cos(m\pi y) \quad (m = 0, 1, \ldots, \infty). \tag{20}$$

The expressions for the expansion coefficients a_m given in (16) are then the standard Fourier-series expressions.

In general, an analytic solution to equation (12) is not readily available. This is certainly true for the case of a logarithmic velocity distribution and the corresponding parabolic diffusivity distribution derived from (6). For this case

$$\chi(y) = 1 + \lambda(1 + \ln y), \tag{21}$$

where $\lambda = u_*/\bar{u}\kappa$, κ is von Kármán's constant and

$$\psi(y) = \frac{1}{\lambda}(1-y)\,y. \tag{22}$$

A number of techniques are available for the solution of boundary-value problems of this type. These include finite-difference methods, expansions using a basis set of complete functions, and variational methods. The procedure employed in this paper is a power-series expansion (Boyce & DiPrima 1969), chosen for its ease of use.

By changing the independent variable to $z = 1-y$, so z measures downwards from the free surface, (11) becomes

$$z(1-z)\frac{\mathrm{d}^2H}{\mathrm{d}z^2}+(1-2z)\frac{\mathrm{d}H}{\mathrm{d}z}+\gamma\lambda[1+\lambda(1+\ln(1-z))]H=0. \tag{23}$$

All of the coefficients of (23) are polynomials in z or functions that may be expanded as polynomials in z, i.e.

$$\ln(1-z) = -\sum_{m=1}^{\infty}\frac{z^m}{m} \quad (0 \leqslant z < 1), \tag{24}$$

and hence a power series in z may be employed to represent the eigenfunction H. The point $z = 0$ is a regular singular point, and so the two linearly independent solutions are given by

$$H_1(z) = \sum_{n=0}^{\infty} b_n z^n \tag{25}$$

and

$$H_2(z) = H_1(z)\ln z + \sum_{n=1}^{\infty} c_n z^n, \tag{26}$$

where the coefficients b_n and c_n are found by direct substitution into (23). The second of these solutions does not satisfy the boundary condition at the free surface, and so may be discarded.

A set of recurrence relations, relating each coefficient b_n to those before it, may be obtained by substituting $H_1(z)$ into (23). These relationships are

$$b_1 = -\theta b_0, \tag{27}$$

$$b_2 = 0.25[(2-\theta)b_1+\phi b_0], \tag{28}$$

$$b_{k+1} = \frac{1}{(k+1)^2}\left[(k^2+k-\theta)b_k+\phi\left(\frac{b_0}{k}+\frac{b_1}{k-1}+\ldots+b_{k-1}\right)\right] \quad (k = 2, \ldots, \infty) \tag{29}$$

where $\phi = \gamma\lambda^2$, $\theta = \gamma\lambda(1+\lambda)$, and b_0 is arbitrary so it may be set equal to unity. An expression, albeit an infinite power series, is now available for the eigenfunction $H(y)$ as a function of the eigenvalue γ.

As the diffusivity $\psi(y)$ vanishes on the boundaries, it is not convenient to use (13) directly to determine the eigenvalues. Instead, the integrated form of (11) incorporating the boundary conditions,

$$\int_0^1 \chi(y)\,H(y)\,\mathrm{d}y = 0, \tag{30}$$

yields a characteristic equation from which the eigenvalues may be evaluated. Although the explicit γ-dependence of (30) is not readily obtained, an iterative process suffices to generate the eigenvalues.

The theory of power-series solutions to ordinary differential equations guarantees that the series will converge in the interval $0 \leqslant z < 1$, but not necessarily at $z = 1$.

This method for obtaining the eigenfunctions and eigenvalues may be applied to any well-behaved diffusivity and velocity distribution. The point in the flow about which the expansion should be made will depend on the form of the diffusivity and velocity.

Equation (15) may now be written as

$$c(x, y) = \sum_{i=0}^{\infty} a_i \exp\left(-\tfrac{1}{8}\gamma_i f x\right) \sum_{n=0}^{\infty} b_{ni} z^n, \tag{31}$$

where the b_{ni} and γ_i are known and the boundary condition at $x = 0$ determines the coefficients a_i.

5. Numerical results

Two computer programs were developed to calculate the eigenvalues and concentration distributions for a range of velocity and diffusivity distributions. A friction factor of 0.08, chosen to be representative of the experimental data presented in §6, was used for all numerical calculations in this section, while von Kármán's constant was taken as 0.35. All computer calculations were performed on a Burroughs 6900 computer.

The initial task of generating the eigenvalues was achieved with the use of the eigenfunction solution described in §4 and (30). Equation (30) represents a function of the parameter γ that possesses an infinite number of discrete positive real roots, and a simple regular false algorithm was employed to obtain the eigenvalues by iteration. This root-finding method was found to be quite satisfactory for this purpose, and, provided that not too large an interval was chosen to contain the eigenvalue, 5-decimal-place accuracy was achieved with less than 8 iterations. Double-precision accuracy was used for all calculations in the program designed to generate the eigenvalues.

The results of this program were easily checked by generating the eigenvalues for problems with known analytic solutions. Two such problems were considered: that for a uniform velocity and uniform diffusivity and that for a uniform velocity and parabolic diffusivity. The eigenfunctions for these distributions are cosine functions, as stated in §4, and Legendre polynomials respectively. In each case 70 terms were used in the power series, and eigenvalues correct to 5 decimal places were obtained for the first seven eigenvalues. To obtain further eigenvalues accurately for the case of uniform velocity and uniform diffusivity more terms in the power series were required. The time required to generate the first 7 eigenvalues for these two cases was typically 3 s. As the eigenfunctions for the second case are finite-degree polynomials, it is not surprising that the power-series solution is efficient and accurate.

Eigenvalues for a logarithmic velocity and parabolic diffusivity were also generated. Owing to the singularity in the velocity, the convergence of the eigenvalues is unlikely to be as rapid as for the two cases considered above. The first 5 eigenvalues calculated using 20, 50, 100, 150 and 200 terms in the series expansion are presented in table 1. To strike a balance between accuracy and efficiency, it was decided to use 70 terms to determine the eigenvalues and eigenfunctions employed in the calculation of the concentration distribution. Although the accuracy of the larger eigenvalues will suffer somewhat by this choice, it was felt that, as these higher-order eigenfunctions decay rapidly as one moves downstream from the source, this sacrifice of accuracy would not be important except very near the origin.

To enable some comparisons to be made a shooting-method solution was also developed. This technique was found to be considerably less efficient than the power-series method presented here, although as it was not refined to any great extent a comparison between the efficiencies of the procedures would be unfair. However,

Terms	γ_1	γ_2	γ_3	γ_4	γ_5
20	7.79986	24.03313	48.70618	81.82070	123.42593
50	7.80148	24.05366	48.79930	82.07270	123.88065
100	7.80135	24.05196	48.79155	82.05074	123.83420
150	7.80127	24.05100	48.78717	82.03829	123.80758
200	7.80123	24.05053	48.78501	82.03216	123.79443

TABLE 1

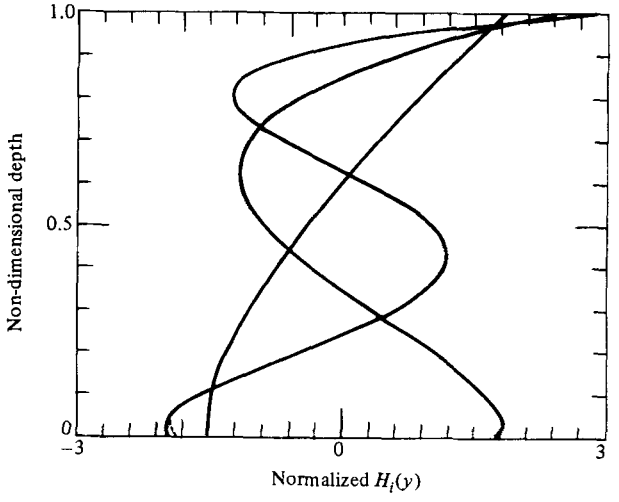

FIGURE 1. The first three normalized eigenfunctions for a logarithmic velocity and parabolic diffusivity with $f = 0.08$ and $\kappa = 0.35$. The solid lines were obtained using 40 terms in the power-series approximation. The dashed lines were obtained using 100 terms in the power-series approximation.

this numerical scheme did confirm the correctness of the eigenvalues generated with the series solution.

The first 3 normalized eigenfunctions for a logarithmic velocity and parabolic diffusivity are plotted in figure 1. As stated in §4 the power-series representations of these functions are guaranteed to converge in the open interval $0 < y \leqslant 1$. The number of terms required to obtain an accurate approximation to the functions will increase near the lower end of the interval, and thus a region near the lower boundary will contain the maximum error in the power-series representation. The solid line in figure 1 was evaluated using 40 terms in the series expansion, and the dashed line using 100 terms. This region of error can be seen to be confined to the bottom 3 or 4 % of the flow.

Figure 2 represents the concentration contours downstream of a rectangular source of width 0.01 centred at $y = 0.75$ in a flow with a logarithmic velocity profile and parabolic diffusivity profile. On the same diagram the concentration contours for the same source but with a power-law velocity $(u/u_{\max} = (y/y_n)^{1/n})$ and the same parabolic diffusivity are shown by the dashed lines. The choice of $n = 3.29$ was made by performing a least-squares power-law fit to the logarithmic velocity distribution above $y = 0.1$. As expected, the two sets of contours are almost indistinguishable. The consequence of this result is that the power-law velocity and logarithmic velocity

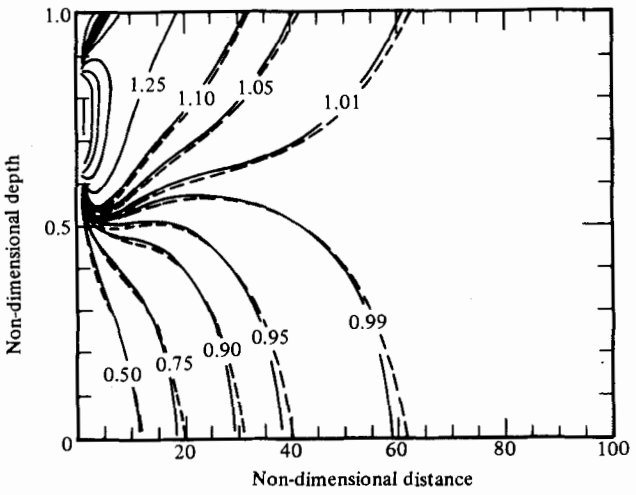

FIGURE 2. The concentration contours downstream from a source at 0.75 above the bed. For this calculation the friction factor was 0.08. The solid lines are for a logarithmic velocity ($\kappa = 0.35$ from measured velocities) and a parabolic diffusivity. The dashed lines are for a power-law velocity ($n = 3.29$ see text) and the same parabolic diffusivity.

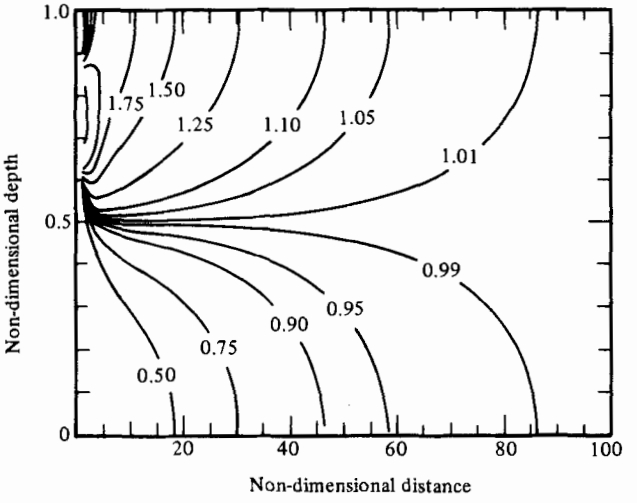

FIGURE 3. The concentration contours downstream from a source at 0.75 above the bed. For this calculation the friction factor was 0.08, the velocity and diffusivity were assumed uniform with the same average value as used in figure 2.

may be confidently interchanged in dispersion calculations provided that the parabolic diffusivity distribution is retained. The power law is advantageous in that it is physically reasonable over the whole flow region and well behaved at the channel bed.

The results for uniform velocity and uniform diffusivity profiles are presented in figure 3. The depth-averaged velocity and diffusivity are the same for figures 2 and 3.

A comparison of these two figures reveals the downstream distance where mixing is 99% complete is predicted to be substantially larger in the flow with uniform velocity and uniform diffusivity. This result, reflected by the first eigenvalues in each

Velocity	Diffusivity	First eigenvalue
logarithmic	parabolic	7.8014
power	parabolic	7.5652
uniform	parabolic	7.0000
logarithmic	uniform	6.3770
uniform	uniform	5.7573

TABLE 2

solution, does depend on the source position, although the reduction in mixing distance predicted by the logarithmic (or power) velocity and parabolic diffusivity is typical of most positions of the release. Table 2 lists the first eigenvalue for various velocity and diffusivity profiles, and allows a comparison between the various approximations to be made. These results suggest that an accurate knowledge of the diffusivity is of greater importance than a knowledge of the velocity in predicting the distance to almost complete mixing. It would be useful to apply this method to wide rivers where the pollutant is well mixed vertically but is spreading horizontally (Smith 1982). However, for this case the importance of the diffusivity distribution is unfortunate, since although it is a relatively easy matter to measure the velocity distribution there is no simple way of determining the diffusivity distribution.

It is possible to find an ideal position for the source which yields a minimum mixing distance. This source position corresponds to the depth where the first eigenfunction vanishes, thus leaving the second eigenfunction to dominate far downstream from the source. As Smith (1982) explains, this source position ensures that the pollutant concentration at the flow boundaries never exceeds the fully mixed concentration. Physically the concentration maximum in the dispersing plume is forced to regions of lower diffusivity and lower velocity, and thus the ideal source position corresponds to the depth where the effect of the velocity shear trying to drag the plume to the bed is exactly balanced by the diffusivity gradient attempting to raise the plume to the surface. The result is that the plume concentration maximum travels horizontally in the flow, never reaching the bed or the free surface. This source position is located at approximately $y = 0.6$ for the logarithmic velocity and parabolic diffusivity.

To facilitate a source at the bed of the flow where the logarithmic velocity is negative, a linear velocity distribution was fitted to the logarithmic velocity. The point of overlap for the two distributions, $y = e^{-1/\lambda}$, was chosen so that the velocities and their gradients were the same. This linear velocity was used together with the eigenfunctions calculated from the logarithmic velocity to evaluate the numerator of (16) and hence the expansion coefficients a_j. Using this linear velocity was not an attempt to include a viscous sublayer at the bed.

6. Experiments

To obtain an approximately two-dimensional flow, a wide (560 mm), shallow (150 mm) and long (15 m) laboratory flume was modified by placing 20 mm by 7 mm 'roughness' strips on the base of the flume. Roughness strips were spaced at 20 mm, creating cavities over 50 % of the bed, perpendicular to the flow direction. This had the effect of destroying the secondary flow and ensuring an approximately two-dimensional flow. However, the extreme roughness dominates close to the bed, and

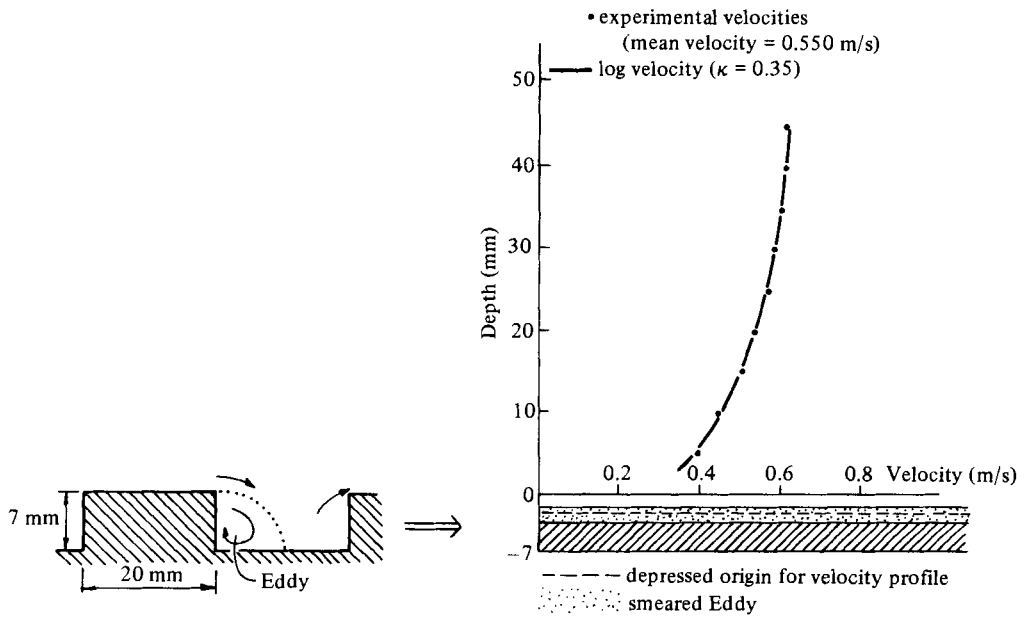

FIGURE 4. The smearing of the bed forms and stationary eddy is shown, together with a typical velocity profile. The depressed origin of the logarithmic velocity is also demonstrated.

therefore the experimental results presented are only for those cases where this region is small relative to the total depth.

A tracer of salt (NaCl) solution was injected into the flume as a continuous line source on either the surface, or the bottom, of the flow. After an initial unsteady period, measurements could be taken at various depths and distances from the source to produce a description of the dispersion pattern. Data was passed from conductivity probes via a salinity meter and data-acquisition system to a PDP11/34 computer for storage and future analysis. The conductivity probes consisted of a hollow 6 mm stainless-steel tube with two platinum electrodes glued into its end. The electrodes were 3.2 mm long, 0.5 mm in diameter and spaced 1.6 mm apart. The probes were placed at an angle of 25° facing into the flow. Sufficient data were collected to enable an analysis of the turbulent concentration fluctuations and to produce an average non-dimensional concentration at each measurement point.

Measured concentrations were non-dimensionalized by subtracting the background concentration and dividing by the fully mixed concentration, both of which were measured during an experimental run. Provided that the probes respond linearly, this technique eliminates the possibility of probe-calibration errors.

Flow parameters (velocities, flow depths, etc.) required by the model were recorded separately for each experimental run. Average velocity profiles were measured across and along the laboratory flume with an 8 mm Pitot tube and a Kent Mini-flow impellor-type meter. The velocity profile shown in figure 4 is typical of the measurements made over the central two-thirds of the flume. The rectangular roughnesses are also shown with this profile. In each cavity a stationary eddy was observed and the approximate geometry of the eddy was recorded. The origin for the velocity distribution law was predicted using the results of previous investigators (Antonia & Wood 1975; Aytekin & Berger 1979) as applied to longitudinally averaged bed conditions. That is, the roughness element and eddy areas were smeared to obtain

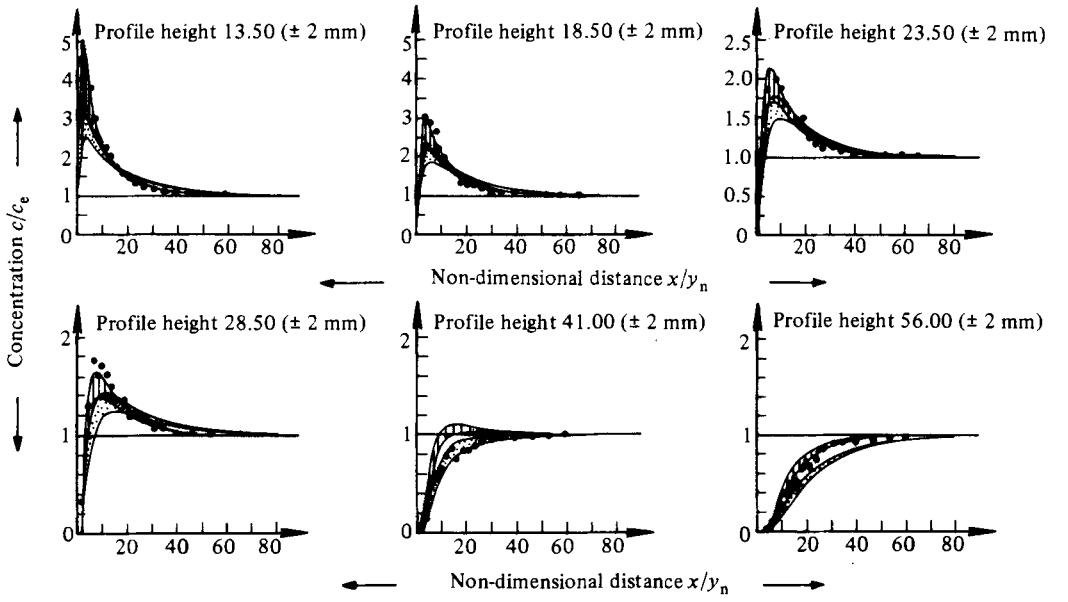

FIGURE 5. A comparison of the concentration distributions of particular depths for: ▥, predictions made with the logarithmic velocity profile and the parabolic diffusivity; ▨, predictions made using a uniform velocity and diffusivity (with the same average values as for the first case); ●, the experimental points. The source was at the bottom of the flow, the friction factor f was 0.072 and the flow depth was 75.6 mm.

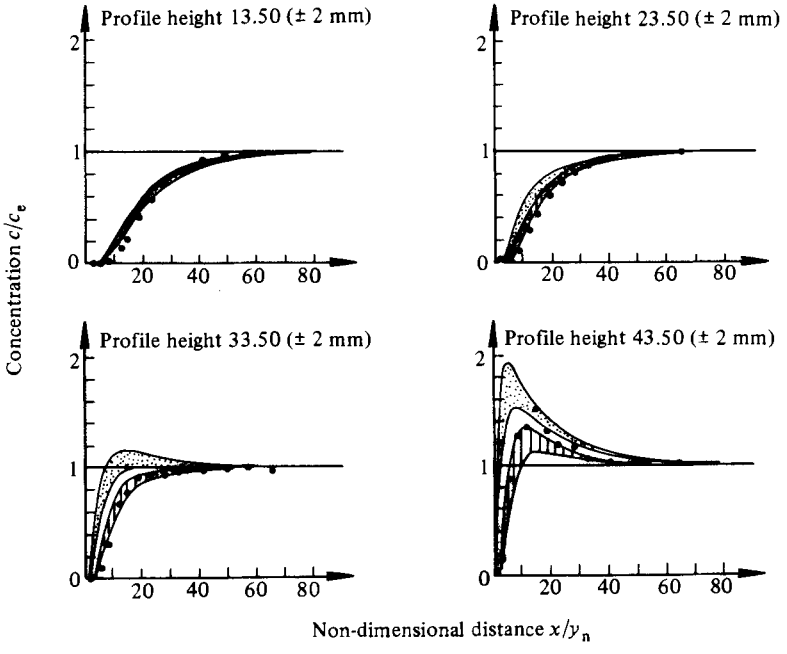

FIGURE 6. A comparison of the concentration distributions of particular depths for: ▥, predictions made with the logarithmic velocity profile and the parabolic diffusivity; ▨, predictions made using a uniform velocity and diffusivity (with the same average values as for the first case); ●, the experimental points. The source was at the bottom of the flow, the friction factor f was 0.087 and the flow depth was 60.2 mm.

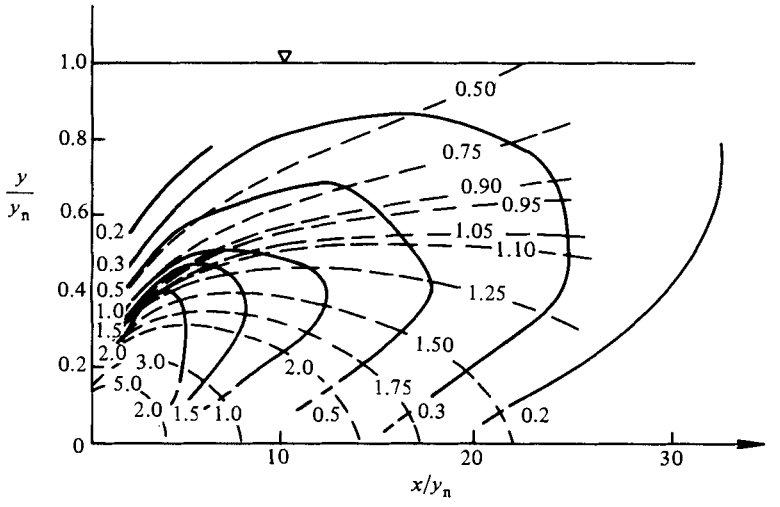

FIGURE 7. A plot of standard deviation of the concentration contours (solid lines) and the mean concentration contours (dashed lines) for a source at the bed. The velocity is logarithmic and the diffusivity parabolic. In this case the friction factor was $f = 0.072$ and the flow depth was 75.6 mm.

an average depth. The origin was then taken as 0.25 of the spread eddy depth below the top of the spread eddy. This process is shown in figure 4. The best logarithmic fit to all experimental velocity data defined in this manner was obtained with $\kappa = 0.35$.

Experimental concentration values, having been calibrated by equilibrium and background concentrations, are plotted on the figures of theoretical curves (figures 5 and 6). The two shaded regions shown in each plot correspond to theoretical concentration profiles for a logarithmic velocity distribution and a uniform velocity distribution. The bounds of each region are given by profiles at 2 mm either side of the measured probe height, representing the accuracy to which the probe height may be determined. Errors in locating the probes arise from fluctuations in the bed position (± 1 mm), measurement of the probe height (± 0.5 mm) and fluctuations of the water surface (± 1 mm).

As can readily be seen from figures 5 and 6, the logarithmic-velocity/parabolic-diffusivity yields better predictions than the uniform-velocity/uniform-diffusivity distribution.

Finally, the salinity data recorded was analysed for the standard deviation of the concentration fluctuations. Since the probes average over an area, the absolute value of the results depends on the size and orientation of the probes. The results, presented in figure 7, must therefore be considered as qualitative only. They do, however, show that close to the source the fluctuations are of the same order as the mean concentration.

R. I. Nokes and A. J. McNulty would like to thank the National Water and Soil Conservation Organisation and the New Zealand Grants Committee for their support while this study was carried out.

REFERENCES

ANTONIA, R. A. & WOOD, D. H. 1975 Calculation of a turbulent boundary layer downstream of a small step change in surface roughness. *Aero. Q.* **26**, 202–210.

AYTEKIN, A. & BERGER, F. P. 1979 Turbulent flow in rectangular ducts with low aspect ratios having one rough wall. *Nucl. Energy* **18**, 53–63.

BOYCE, W. E. & DIPRIMA, R. C. 1969 *Elementary Differential Equations and Boundary Value Problems*. Wiley.

COUDERT, J. F. 1970 A numerical solution of the two-dimensional diffusion equation in a shear flow. *W. M. Keck Lab. of Hydraulics and Water Research, Tech. Memo.* 70–7, *California Institute of Technology*.

FISCHER, H. B., LIST, E. J., KOH, R. C. Y., IMBERGER, J. & BROOKS, N. H. 1979 *Mixing in Inland and Coastal Waters*. Academic.

HOLLEY, E. R., SIEMANS, J. & ABRAHAM, G. 1972 Some aspects of analysing transverse diffusion in rivers. *J. Hydraul. Res.* **10**, 27–57.

INCE, F. L. 1927 *Ordinary Differential Equations*. Longman's, Green.

MCNULTY, A. J. & WOOD, I. R. 1984 A new approach to predicting the dispersion of a continuous pollutant source. *J. Hydraul. Res.* **22**, 23–34.

SMITH, R. 1982 Where to put a steady discharge in a river. *J. Fluid Mech.* **115**, 1–11.

YEH, G. T. & TSAI, Y. T. 1976 Dispersion of water pollutants in a turbulent shear flow. *Water Resources Res.* **12**, 1265–1270.